Evolution of relaxor ferroelectric behavior of poly(vinylidene fluoride trifluoroethylene chlorofluoroethylene) terpolymer nanorods

Jun-Hong Lin, S. G. Lu, M. Lin, Markus Geuß, and Q. M. Zhang

Related Articles

Additional information on Appl. Phys. Lett.

Evolution of relaxor ferroelectric behavior of poly(vinylidene fluoride trifluoroethylene chlorofluoroethylene) terpolymer nanorods

Jun-Hong Lin,[1,2] S. G. Lu,[2] M. Lin,[2] Markus Geuβ,[3] and Q. M. Zhang[1,2,4,a)]

[1]*Department of Materials Science and Engineering, The Pennsylvania State University, University Park, Pennsylvania 16802, USA*
[2]*Materials Research Institute, The Pennsylvania State University, University Park, Pennsylvania 16802, USA*
[3]*Max-Plank-Institute for Microstructure Physics, Weinberg 2, D-06120 Halle, Germany*
[4]*Department of Electrical Engineering, The Pennsylvania State University, University Park, Pennsylvania 16802, USA*

The evolution of relaxor ferroelectric behavior of poly(vinylidene fluoride trifluoroethylene chlorofluoroethylene) [P(VDF-TrFE-CFE)] terpolymer nanorods with diameters reduced from 200 to 25 nm was investigated. It was observed that all the nanorods studied exhibited relaxor ferroelectric behavior, as characterized by the dielectric peak shifting toward high temperatures with increasing frequency. The frequency-permittivity peak temperature characteristics fit well with the Vogel–Fulcher (VF) relation. Moreover, the freezing temperature in the VF relation decreased with the reduction of nanorod diameter, indicating that the scaling down of the lateral size of nanorods influenced the relaxor ferroelectric behavior of the terpolymer. © *2009 American Institute of Physics*. [DOI: 10.1063/1.3182786]

Ferroelectric materials are strongly coupled materials and consequently their properties and responses can be sensitive to system sizes as they approach nanometer scale.[1–7] Relaxor ferroelectrics are a special class of ferroelectrics whose dielectric responses are dominated by the glasslike polar-nonpolar transition process. It is of great interest to investigate how the relaxor ferroelectric behavior evolves as the system size becomes small.[8–10] In this letter, we study the relaxor ferroelectric terpolymer nanorods, poly(vinylidene fluoride trifluoroethylene chlorofluoroethylene) P(VDF-TrFE-CFE) 59.2/33.6/7.2 mol %, which can be prepared via a melting-wetting process on an anodized aluminum oxide (AAO) template.[11,12] The terpolymer nanorods with diameters of 25, 70, and 200 nm were prepared and investigated.

The terpolymer nanorods were fabricated using alumina templates with nanopore sizes of 25, 70, and 200 nm diameter, respectively. Alumina templates with these nanopore diameters were prepared following the established fabrication processes.[13–16] The AAO templates were cleaned with deionized water thoroughly, and then were heated at 400 °C for 4 h to remove the moisture and other impurities. It was found that this procedure of removing impurities in the nanopore templates is crucial in order to measure the dielectric properties of the terpolymer nanorods. Residual impurities in nanopore templates can cause severe conduction loss, which may dominate the dielectric properties. In order for the terpolymer to infiltrate into the nanopores of the templates, a two-step infiltration process was developed. First, the solution of 3 wt % P(VDF-TrFE-CFE) dissolved in dimethyl formamide was poured to the top surface of the AAO nanopore template and the solvent was evaporated at room temperature. After that, the terpolymer with templates was heated at 260 °C for 4 h in a temperature controlled vacuum oven, and then cooled down to room temperature at a rate of 1 °C/min. The excess terpolymer on the top of the AAO templates was removed by mechanical polishing with 1 μm sized alumina powders. The bottom of AAO template was opened by first removing the aluminum layer with 1.7 wt % $CuCl_2$ solution with $HCl:H_2O=1:1$ followed by etching with 10 wt % H_3PO_4 at 30 °C to remove alumina buffer layer. For electrical characterization, Au electrodes were sputtered.

The microstructures of the nanorods were evaluated by x-ray diffraction (XRD), as schematically shown in Fig. 1(a), using a Philips X'Pert Pro Cu $K\alpha$ diffractometer with an x-ray wavelength of 0.15406 nm. Morphologies of the nanorods were observed using a field emission scanning electron microscope (SEM) (LEO 1530) and a transmission electron microscope (TEM) (JEOL JEM 1200 EXII). Dielectric characterization was carried out by an *LCR* meter (HP4284A) equipped with a computer controlled temperature chamber.

Presented in Fig. 1(b) is a SEM image of an AAO template with 70 nm diameter pores. From the SEM image, it can be deduced that the nanopore area is 31.6% of the total surface area (or 31.6% of the total volume is occupied by the nanopore). The volume percentage of nanopores in the template is 37.4%, 31.6%, and 36.8% for the nanopore sizes of 25, 70, and 200 nm diameter, respectively. Figure 1(c) is a SEM image of the alumina template infiltrated with the terpolymer. After etching away the alumina template, the free standing terpolymer nanorods were imaged by SEM, as shown in Fig. 1(d). Figure 1(e) is the TEM image of the 70 nm nanorod.

The XRD profiles at diffraction angles near the (110, 200) peak for the nanorods in templates, as well as the bulk film, are presented in Fig. 2. Earlier studies have demonstrated that the crystal growth for PVDF and its copolymers in 200 nm diameter nanopores shows orientation with the polymer chains oriented perpendicular to the pore walls.[12] Therefore, even with a 36.8 vol % of terpolymer in the AAO

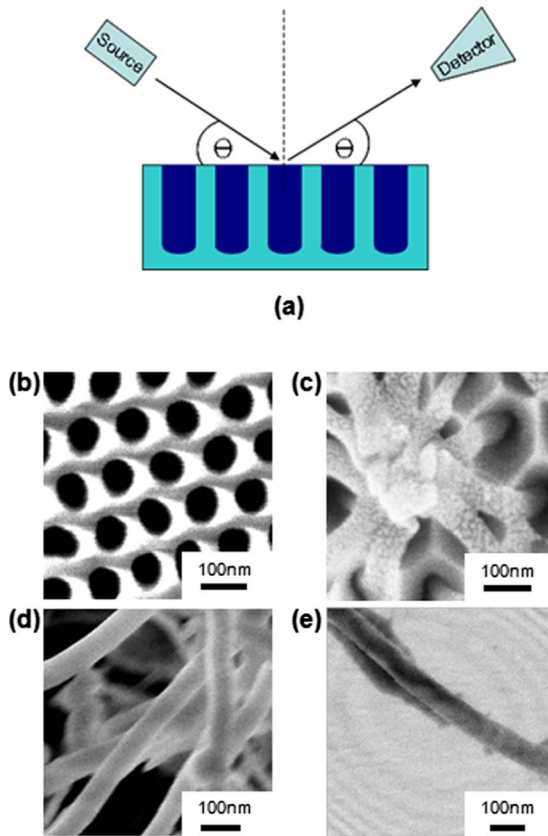a)Electronic mail: qxz1@psu.edu.

95, 022911-1

FIG. 1. (Color online) Schematic diagram of XRD setup, SEM, and TEM images for nanorods of 70 nm diameter with template. (a) Schematic diagram of XRD setup; (b) template (SEM); (c) nanorods and template (SEM); (d) freestanding nanorods (SEM); and (e) nanorod (TEM). Scale bar = 100 nm.

template, the 200 nm diameters terpolymer nanorods also display a sharp diffraction peak. However, the x-ray data from the 70 nm diameter nanorods show quite different features. Although the volume fraction of terpolymer nanorods
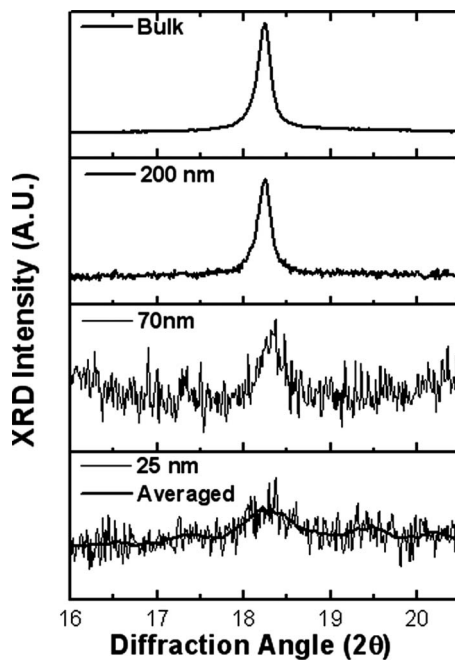

FIG. 2. XRD profiles at diffraction angles near (110, 200) for 25, 70, and 200 nm diameter P(VDF-TrFE-CFE) nanorods and bulk terpolymer film.
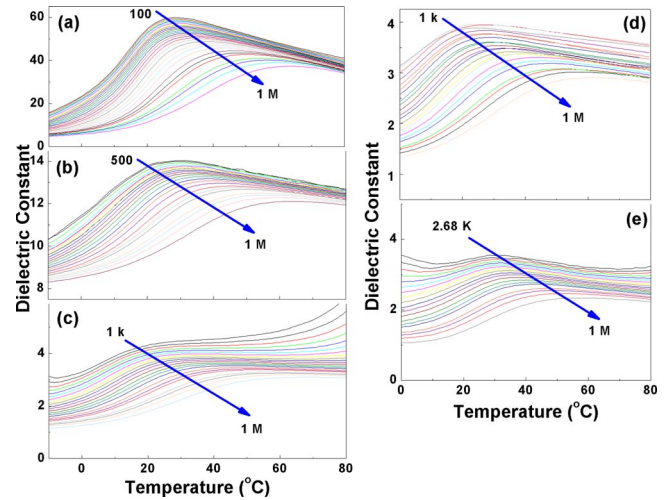

FIG. 3. (Color online) Dielectric constant at different frequencies vs temperature for P(VDF-TrFE-CFE) terpolymer (a) bulk film. (b) Nanorods of 200 nm diameter. (c) Nanorods of 70 nm diameter without the subtraction of conduction background. (d) Nanorods of 70 nm diameter after the subtraction of conduction background. (e) Nanorods of 25 nm diameter.

in the 70 nm diameter pore size template does not differ much from that in the 200 nm template, the x-ray peak intensity of 70 nm nanorods is significantly reduced. Moreover, the crystallite size along the (110, 200) orientations (perpendicular to the polymer chains), as deduced from the x-ray peak width, is also reduced ($L_{(110,200)}$ = 34.8 ± 5.3 nm) in 70 nm diameter terpolymer nanorods. $L_{(110,200)}$ is derived from the Scherrer's formula[17]

$$L_{(110,200)} = \frac{0.9\lambda}{B \cos \theta}, \quad (1)$$

where λ is the x-ray wavelength, B is the full width at half maximum of the x-ray peak, and θ is the diffraction angle. In comparison, $L_{(110,200)}$ for the bulk film and for the 200 nm diameter nanorods are 67.9 ± 1.2 and 67.0 ± 2.4 nm, respectively. For samples with 25 nm diameter nanorods, the x-ray data show a weak diffraction peak with an even broader peak width, indicating a very small crystallite size $L_{(110,200)}$ ×(=13.7 ± 2.7 nm) in the 25 nm terpolymer nanorods. The very weak x-ray peaks for 25 and 70 nm terpolymer nanorods indicate low crystallinities in these terpolymer nanorods.

The dielectric properties of the bulk terpolymer films are presented in Fig. 3(a). The terpolymer exhibits typical relaxor ferroelectric behavior. That is, the dielectric constant peak shifts progressively toward higher temperatures with increasing frequency and this shift of dielectric constant peak temperature with frequency can be described well with the empirical VF relation, i.e.,[8–10,18,19]

$$f_m = f_0 \exp\left(-\frac{U}{k(T_m - T_f)}\right), \quad (2)$$

where f_m is the frequency of the dielectric constant peak at the temperature T_m, f_0 is the pre-exponential factor, U is the activation energy, and T_f is the static freezing temperature. The fitting to the bulk film using Eq. (2) is presented in Fig. 4, which yields a T_f = 21.24 ± 0.25 °C. The fitted results are summarized in Table I.
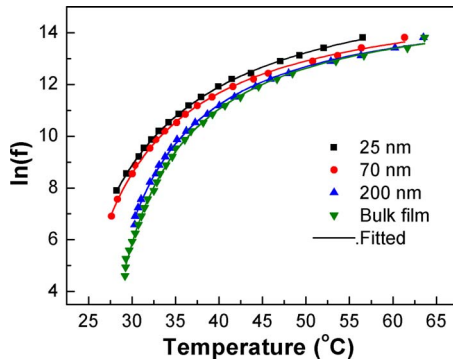
FIG. 4. (Color online) Logarithmic frequency vs permittivity peak temperature data for 25, 70, and 200 nm diameter terpolymer nanorods and bulk film. The solid lines are fitted according to the VF relation.

For the 200 nm diameter nanorods, the dielectric properties deduced from the alumina template-terpolymer composite are shown in Fig. 3(b). Since terpolymer nanorods and alumina template are dielectrically in parallel, the total dielectric constant ε is the summation of the two dielectric constants ε_{Terp}, the dielectric constant of terpolymer nanorods, and ε_{Al} ($\sim$10) of alumna, times their respective volume fraction α_{Terp} and α_{Al}, as shown in Eq. (3)

$$\varepsilon = \alpha_{Terp}\varepsilon_{Terp} + \alpha_{Al}\varepsilon_{Al}. \quad (3)$$

Fitting the shift of the dielectric constant peak with frequency for the 200 nm diameter nanorods with the VF relation yields a $T_f = 20.83 \pm 0.41$ °C. This T_f value, although slightly lower than that of the bulk film, is still nearly the same. Besides T_f, all the other VF fitting parameters for the 200 nm diameter nanorods are nearly the same as those of the bulk film within the error bar (see Table I).

The dielectric constant for 70 and 25 nm diameter nanorods is presented in Figs. 3(c) and 3(e), respectively. As can be seen, due to much lowered crystallinity in the terpolymer nanorods, the dielectric peak becomes much weaker compared with that of 200 nm nanorods. Due to the increased contribution from the conduction loss, which increases with temperature, some of the dielectric curves do not show clear dielectric peaks especially for the data of 70 nm diameter nanorods. To extract the peak position from the experimental data, we assume that the overall peak shape of the 70 nm nanorods after the subtraction of conduction background, as well as that from the alumina template, be similar to that of 200 nm nanorods. Based on this assumption, the background dielectric constant in the temperature range investigated is taken as $\varepsilon_b = a + bT$, where T is the temperature and a and b are constants from the fitting to the dielectric data of 70 nm

nanorods and 200 nm nanorods. In this procedure, the background dielectric data at the two temperature ends (-10 and 80 °C) of the dielectric constant curve of the 70 nm diameter nanorods is fitted as $a_1 + b_1T$ and at the two temperature ends of the 200 nm diameter nanorods data as $a_2 + b_2T$, from which $a = a_1 - a_2$ and $b = b_1 - b_2$ are obtained. Dielectric data after the subtraction for the 70 nm diameter nanorods are presented in Fig. 3(d), from which, the shift of the dielectric peak with frequency can be determined and the fitting with VF law yields a $T_f = 16.71 \pm 0.45$ °C, which is lower than that of the bulk film and 200 nm nanorods. Both the pre-exponential factor f_0 and activation energy are larger than those of the bulk film (see Table I).

The dielectric data for 25 nm diameter nanorods display broad dielectric constant-temperature peaks. The fitting of the data with VF relation, as presented in Fig. 4, yields a $T_f = 14.49 \pm 0.37$ °C, which is further lowered compared with 70 nm nanorods. The activation energy, $U = 1.03 \times 10^{-2}$ eV, for 25 nm terpolymer nanorods is higher than other nanorods and bulk film, suggesting increased energy barriers for the nanopolar domain reorientation for the terpolymer in confined nanorod systems.

In summary, it was found that the relaxor ferroelectric behavior persists in the terpolymer nanorods in AAO nanopores with diameter down to 25 nm. On the other hand T_f the freezing temperature of VF relation, moves to lower temperature and the activation energy (U) becomes higher as the nanorod diameter is reduced to 25 nm. The observed changes in the nanorod systems can be caused by several effects, such as the reduced crystallite size and/or the interface effect.[2–6]

TABLE I. Summary of the fitted results using the VF relation.

Nanorod diameter (nm)	U (eV)	f_0 (Hz)	T_f (°C)
25	1.03×10^{-2}	16.32×10^6	14.49
70	8.29×10^{-3}	7.27×10^6	16.71
200	7.08×10^{-3}	5.43×10^6	20.83
Bulk	7.33×10^{-3}	5.87×10^6	21.24

[1]K. Ishikawa, K. Yoshikawa, and N. Okada, Phys. Rev. B **37**, 5852 (1988).
[2]A. Rudiger, T. Schneller, A. Roelofs, S. Tiedke, T. Schmitz, and R. Waser, Appl. Phys. A: Mater. Sci. Process. **80**, 1247 (2005).
[3]M. H. Frey and D. A. Payne, Phys. Rev. B **54**, 3158 (1996).
[4]S. G. Lu, C. L. Mak, and K. H. Wong, J. Am. Ceram. Soc. **84**, 79 (2001).
[5]S. Li, J. Eastman, Z. Li, C. Foster, R. E. Newnham, and L. E. Cross, Phys. Lett. A **212**, 341 (1996).
[6]H. W. Qu, W. Yao, T. Garcia, J. D. Zhang, A. V. Sorokin, S. Ducharme, P. A. Dowben, and V. M. Fridkin, Appl. Phys. Lett. **82**, 4322 (2003).
[7]A. V. Bune, V. M. Fridkin, S. Ducharme, L. M. Blinov, S. P. Palto, A. V. Sorokin, S. G. Yudin, and A. Zlatkin, Nature (London) **391**, 874 (1998).
[8]L. E. Cross, Ferroelectrics **76**, 241 (1987).
[9]D. Viehland, S. Jang, L. E. Cross, and M. Wuttig, J. Appl. Phys. **68**, 2916 (1990).
[10]Q. M. Zhang, V. Bharti, and X. Zhao, Science **280**, 2101 (1998).
[11]M. Steinhart, J. H. Wendorff, A. Greiner, R. B. Wehrspohn, K. Nielsch, J. Schilling, J. Choi, and U. Gösele, Science **296**, 1997 (2002).
[12]M. Steinhart, P. Göring, H. Dernaika, M. Prabhukaran, U. Gösele, E. Hempel, and T. Thurn-Albrecht, Phys. Rev. Lett. **97**, 027801 (2006).
[13]A. P. Li, F. Muller, A. Birner, K. Nielsch, and U. Gösele, J. Appl. Phys. **84**, 6023 (1998).
[14]H. Masuda, K. Yada, and A. Osaka Jpn, J. Appl. Phys., Part 2 **37**, L1340 (1998).
[15]O. Jessensky, F. Muller, and U. Gösele, Appl. Phys. Lett. **72**, 1173 (1998).
[16]H. Masuda and K. Fukuda, Science **268**, 1466 (1995).
[17]A. L. Patterson, Phys. Rev. **56**, 978 (1939).
[18]V. Bobnar, B. Vodopivee, A. Levstik, Z. Y. Cheng, and Q. M. Zhang, Phys. Rev. B **67**, 094205 (2003).
[19]Q. M. Zhang, Z. Y. Cheng, and V. Bharti, Appl. Phys. A: Mater. Sci. Process. **70**, 307 (2000).